HHS Public Access

Author manuscript

Cardiovasc Eng Technol. Author manuscript; available in PMC 2016 December 01.

Published in final edited form as:

Cardiovasc Eng Technol. 2015 December ; 6(4): 533–545. doi:10.1007/s13239-015-0236-8.

Development of a Cyclic Strain Bioreactor for Mechanical Enhancement and Assessment of Bioengineered Myocardial Constructs

Betsy H. Salazar[1], **Avery T. Cashion**[2], **Robert G. Dennis**[2], and **Ravi K. Birla**[1]

[1]Department of Biomedical Engineering, University of Houston, Houston, TX

[2]Joint Department of Biomedical Engineering, University of North Carolina/North Carolina State University, Chapel Hill, NC

Abstract

Purpose—The purpose of this study was to develop enabling bioreactor technologies using a novel voice coil actuator system for investigating the effects of periodic strain on cardiac patches fabricated with rat cardiomyocytes.

Methods—The bioengineered muscle constructs used in this study were formed by culturing rat neonatal primary cardiac cells on a fibrin gel. The physical design of the bioreactor was initially conceived using Solidworks to test clearances and perform structural strain analysis. Once the software design phase was completed the bioreactor was assembled using a combination of commercially available, custom machined, and 3-D printed parts. We utilized the bioreactor to evaluate the effect of a 4-hour stretch protocol on the contractile properties of the tissue after which immunohistological assessment of the tissue was also performed.

Results—An increase in contractile force was observed after the strain protocol of 10% stretch at 1Hz, with no significant increase observed in the control group. Additionally, an increase in cardiac myofibril alignment, connexin 43 expression, and collagen type I distribution were noted.

Conclusion—In this study we demonstrated the effectiveness of a new bioreactor design to improve contractility of engineered cardiac muscle tissue.

Keywords

Biomedical Transducers; Microcontrollers; Printed Circuits; Micropositioning Voice-Coil Actuator; Cardiac Tissue Engineering; Artificial Heart Muscle; Bioreactors

Corresponding Author: Ravi K. Birla, PhD, Associate Professor, Department of Biomedical Engineering, Cullen College of Engineering, University of Houston, Houston, TX, 77204, Science and Engineering Research Center (SERC), 3605 Cullen Blvd, Rm. 2021, rkbirla@uh.edu, Ph: 713-743-8861.

Conflict of Interest:

Betsy H. Salazar, Avery T. Cashion, Robert G. Dennis, and Ravi K. Birla declare that they have no conflict of interest.

The Institutional Animal Care and Use Committee (IACUC) at the University of Houston, approved all animal protocols in accordance with the “Guide for the Care and Use of Laboratory Animals” (NIH publication 86-23, 1986).

No human studies were carried out by the authors for this article.

1. Introduction

In 2008, approximately 1 out of 6 deaths in the United States were caused by coronary heart disease [1]. The heart is a complex organ that requires near perfect timing and operation of many intricate parts in order to function properly. The myocardium consists of three major types of cardiac muscle fibers: atrial muscle, ventricular muscle, and excitatory or conductive muscle. The fibers are arranged in two distinct latticeworks generally referred to in literature as the atrial and ventricular syncytia [2]. Under normal conditions, the excitatory heart contraction signal is generated at the sinoatrial (SA) node and spread diffusely through the atrial syncytium causing atrial contraction. The excitatory signal reconvenes at the atrioventricular (AV) node from which it spreads throughout the ventricular syncytium and causes the systolic stroke of the heart pump. Fibrillations in this stepwise rhythm are commonly caused by ischemic conditions in sections of the syncytia where coronary arteries are narrowed or blocked leading to heart muscle damage from oxygen depravation. To improve the function of the infarcted myocardium several different approaches have been and will continue to be studied.

Currently the most prevalent and effective treatment for myocardial infarction is limiting tissue damage by minimizing the length of time an arterial obstruction remains in place. Methods, such as the use of thrombolytics, blood thinners, vascular stents, and bypass surgeries are all effective treatments for blockage in the arteries, however, the necrotic myocardial tissue is most often permanently damaged. Ventricular assist devices can be used to aid the heart pump blood, however, invariably, the gradual increase of non-contractile scar tissue leads to heart failure unless regular maintenance surgeries are performed [3]. Currently heart transplantation is the only standard clinical practice in place to effectively treat infarcted tissue [4]. Conversely, experimental approaches are being studied to develop new and effective treatments. One such method involves the use of stem cells. These cells are undifferentiated cells that can differentiate into specialized cells that aid in the regeneration of damaged tissue. While the heart has been shown to contain populations of these types of cells [4–8], the average rate of regeneration is estimated to be less than 1% turnover annually [9]. This makes stem cell transplantation a logical research endeavor [4], still clinical trials focusing on direct cell injection have not lead to a significant recovery of cardiac function as of yet [3]. Other experimental approaches include heart geometry modifications with biomaterial restraints [10–14], in-situ injectable scaffolds with cardiac cells [15–19], and cardiac muscle constructs cultured in-vitro and implanted on the epicardial surface of the heart [20–26].

One of the most promising and practical aforementioned experimental methods is the fabrication of 3-D artificial heart muscle (3D-AHM) for improving lost functionality of the infarcted myocardium. Thus, the primary focus of heart muscle tissue engineering is to create a clinically relevant graft to restore, supplant, or strengthen the damaged sections of the myocardium [27–29]. For an engineered construct to successfully improve the function of the damaged tissue, it must closely resemble tissue of the native heart, conduct and disseminate electrical impulses, and generate contractile forces equivalent to those found in an adult phenotype tissue [3, 30]. In our laboratory extensive research has been performed to advance artificial heart muscle and other cardiovascular models [31–36]. There are also

several models to support the fabrication of myocardial tissues developed by other investigators [37–44]. The most common strategy is based on the use of a complex 3D scaffold in which primary cardiac cells yield a heart muscle construct. As investigators continue to advance models for bioengineered cardiac muscle, it becomes imperative to establish the best culturing protocols to drive the development of constructs that closely resemble native tissues, not only in function, but in phenotype as well.

With the intent of fabricating 3D-AHM that closely resembles in function and structure native mammalian tissue, different types of bioreactors are used to provide a controlled environment for physiological conditioning. Mechanical stretch, electrical stimulation, and media perfusion are some examples of conditioning used for tissue construct development and maturation. More specifically, mechanical stimulus has been shown to enhance the function of 3D-AHM [45–49]. Cells in native heart muscle are continuously extending and contracting, which provides the tissue with the mechanical stimulation crucial for cardiac function [27]. Therefore conditioning of the fabricated myocardium in vitro is of utmost importance. The current study addresses the need to develop a novel bioreactor to provide mechanical stimulation to 3D-AHM.

Previous studies have assessed the effect of mechanical stimulation of bioengineered heart tissues[45, 46, 48, 50]. Akhyari et al. used the Bio-stretch apparatus to show that a 20% strain at 80 cycles/min (1.33Hz) for a 14-day period yields an increase in tensile strength and cell distribution improvement [45]. In a separate study Fink et al. applied a 20% stretch protocol at 1.5Hz frequency to demonstrate an increase in active force of cardiac constructs after 6 days and mechanical stimulus [46]. Birla et al. developed a bioreactor to support the viability of bioengineered heart muscle by providing 10% stretch at a frequency of 1Hz [50]. Although there have been studies on the enhancement of functional performance brought on by mechanical stimulus, this subject has neither been exclusively nor extensively explored. A review of the literature has lead the authors to determine that the field has matured to a point where it would benefit from the development of a bioreactor that is better suited for the stimulation of 3D-AHM. The work presented on this manuscript focuses on the feasibility and practicality of using our current bioreactor to sustain the viability of 3D-AHM, as well as improve the contractile performance of the tissues.

2. Materials and Methods

2.1 Theory of Bioreactor Operation

Strain is applied to the cardiac muscle constructs using a very low friction and low hysteresis linear voice coil actuator (VCA) apparatus similar to one described elsewhere [51]. The principle of our VCA system is depicted in Fig. 1(a). Lorentz forces are generated orthogonal to the direction of the static magnetic field and to the direction of charge flow through a suspended wire [52]. The force magnitude is proportional to the total length of wire (l), the magnetic field strength (B), and the electrical current (i) as is represented by the following cross product:

$$\mathrm{F}_{\mathrm{Lorentz}} = \mathrm{il} \times \mathrm{B} \quad (1)$$

Tightly coiling the wire increases the total length within the magnetic field. The two sides of the coil are suspended in opposite static magnetic field directions to accomplish a unilateral net force direction. Thus, the magnetic field strength and length of wire are set initially and maintained constant making current the only variable governing the Lorentz force magnitude and direction.

The coil of wire is suspended in the magnetic field by a flexible ABS plastic armature, which acts as a spring under elastic deformation. In static conditions the spring force exactly balances the Lorentz force, which allows for precise linear control of the coil position by modulating the electrical current. Figure 1(b) shows a SolidWorks representation of a frictionless sensor we modified from a previous design [53] to monitor position in this system. Two infrared light sources are directed at two detectors of the relevant wavelength. An interrupter attached to the VCA armature moves within the sensor space proportionally to the movement of the end effector. Position is accurately tracked by observing the differential activations of the two detectors.

2.2 Bioreactor Mechanical Development

The SolidWorks design and assembly as well as an image of the VCA bioreactor are presented in Fig. 2. The mechanical design was originally developed in SolidWorks in order to preserve time and materials by most effectively eliminating clearance errors prior to construction. After the software design phase, rapid manufacturing techniques were employed to produce the bioreactor.

The baseplate was laser cut from a 0.75cm thick piece of poly(methyl methacrylate) stock acrylic. During laser cut manufacturing, holes were placed in appropriate locations for mounting the electronics, the VCA armature, and the magnet housing. Additionally, a circle was cut near the end effector for ideal placement of a standard 35mm culture plate.

The VCA armature was designed to elastically deform in such a way that allows very near uniaxial movement at the end effector. The action of the resulting mechanism is similar to a spring-loaded four-bar linkage. The armature design includes an appropriately sized slot for the coil bobbin to snap in place. A SolidWorks displacement study was executed to test clearances and to set the proportional movement of the beam interrupter to the end effector [figure 2(a)]. The bobbin and the armature were 3D printed out of ABS plastic and mounted to the acrylic baseplate. A 150-turn coil of 36-AWG wire was wound around the bobbin and then snapped into the armature slot.

The permanent magnet housing was constructed by machining low carbon flat-stock steel. A set of four 1.9cm square neodymium N42 rare earth magnets was used to set up the static magnetic field within the housing. After assembly around the armature, the magnet housing was attached to the baseplate using steel 4–40 screws. The optoelectronic sensor was fitted over the beam interrupter using a 1.3cm threaded nylon spacer.

2.3 Electronics

The schematic, printed circuit board design of the electronics developed for this system is shown in figure 3. The circuit is part of an inter-integrated circuit (I2C) digital network

where it can be connected to other bioreactors, sensors, and a custom data acquisition (DAQ) module. The DAQ bidirectionally communicates via USB with a computer running a program written in VisualBasic 2010 for setting stimulation parameters. The DAQ acts as the I2C master device and can independently address each individual VCA bioreactor on the network for parallel experiments. For the purposes of this manuscript, the data presented was obtained from only one bioreactor. Additionally, an embedded PIC18F4550 microcontroller is used for digital communication, armature position monitoring, and stimulus generation.

The VCA is driven using a digital H-Bridge circuit composed of N-Ch (Digikey: IRLZ44) and P-Ch (IRF4905) MOSFETS. The microcontroller setting of the pins labeled A, B, C, and D in the figure 3 schematic controls the direction of current through the coil and therefore direction of armature movement. The magnitude of the coil current is controlled by a 16-bit digital to analog converter (Digikey: DAC8411) attached to the base pin of a NPN power transistor (Digikey: TIP3055).

To mark the end of travel, each IR detector in the position sensor assembly shows variance of a direct current voltage from 0 to 5 volts. In order to calculate the differential activation, two 16-bit analog to digital converters (Digikey: TLC4545) digitize each detector voltage. The difference between the voltages is calculated in the microcontroller firmware. For each position update, this process is repeated 5 times and the median difference is used.

2.4 Calibrations

In order to relate the positional sensor signal with physical length, sensor increments were correlated with the displacements of a linearly variable differential transformer (Schaevitz Sensors: DC-SE1000). The resultant linear relationship from this calibration dataset yielded an R^2 value of 0.9964 and a slope magnitude of 0.0097 mm per sensor increments, which gives a sensor resolution of just under 1μm [Fig. 4(a)].

To calibrate the electrical current to Lorentz force relationship, the VCA armature was held firmly in the home position by a force transducer (Wagner model FDI: 5471885). Force measurements were recorded as coil current was gradually increased [Fig. 4(b)]. The r^2 value was 0.9994 and the slope was 0.0041 yielding a relationship of approximately 4mN per mA.

In each static condition, the spring force exactly balances the Lorentz force, which means that information from the first two calibrations can be used to calculate the spring constant of the VCA armature [Fig. 4(c)]. The VCA was allowed to move freely and the position sensor was monitored as coil current was gradually increased. The spring force to spring displacement relationship has an r^2 value of 0.9992 and slope of 72.49N/m, which by Hooke's law is also the spring constant. Because this system is capable of measuring the cardiac patch twitch forces, knowledge of the spring constant is necessary. This parameter of the bioreactor will be evaluated in depth in subsequent studies. Multiplying the spring constant by the positional sensor precision yields a force resolution in this system of approximately 70μN. This resolution could be optimized by minimizing the spring constant

and also by increasing the proportional movement of the beam interrupter to the end effector.

2.5 Isolation of Neonatal Cardiac Myocytes

Neonatal cardiac cells were isolated from the hearts of 2 to 3 day old Sprague-Dawley rats utilizing a pre-established method [32]. Each heart was cut into 3 to 4 sections in ice-cold PBS phosphate buffer. All the pieces were gently rinsed to remove blood cells and thereupon transferred to a secondary phosphate buffer solution for additional mincing. Tissues were minced into $1mm^2$ fragments and transferred to a dissociation solution (DS) consisting of 0.32mg/mL collagenase type 2-filtered (Worthington Biochemical Corporation, Lakewood, NJ) and 0.6mg/mL pancreatin in phosphate buffer. The minced tissues and 15mL of DS were placed in an orbital shaker for 30 minutes at 37°C and 60 rpm to initiate serial digestion. Once the 1^{st} digestion was completed, the supernatant was collected in 3mL of horse serum in order to neutralize the enzyme, and placed in a centrifuge at 1000rpm for 5 minutes at 4°C. The cell pellet was re-suspended in 5mL of horse serum and kept in an incubator at 37°C supplied with 5% CO_2. Fresh DS was added to the partially digested tissue and the procedure for the digestion was repeated 2 to 3 times. The cells acquired during the serial digestion were pooled, centrifuged and suspended in culture medium (CM). The CM used consists of M199 (Life Technologies, Grand Island, NY) along with 20% F12K (Life Technologies), 10% fetal bovine serum, 5% horse serum, 1% antibiotic-antimycotic, 40ng/mL hydrocortisone, and 100ng/mL insulin. Cell viability was determined by Trypan blue (4%) staining according to the manufacturer's protocol.

2.6 Preparation of the Plates

Each 35mm tissue culture plate was coated with 2mL of SYLGARD (PDMS, type 184 silicone elastomer) (Dow Chemical Corporation, Midland, MI). The PDMS mix used contains a 10:1 ratio of base polymer to curing agent. The silicone elastomer used does not require exothermic cure, therefore the plates were air dried for 2 weeks to prevent any residual chemicals that may be harmful to the cells before sterilization with 80% ethanol. 4 minutien pins (Fine Science Tools, Foster City, CA) 0.1mm in diameter, were then placed in the culture plate to form a 20mm X 20mm square.

2.7 Formation of the Fibrin Gel and Cell Plating

Fibrin gel was formed by adding 1mL of CM containing 10U/mL thrombin to the coated surface of each culture plate. Afterwards, 500μL of saline containing 20mg/mL fibrinogen was added. The culture plates were shaken well to ensure complete mixing of both solutions and complete plate coverage. Subsequently, the plates were placed in the incubator to promote the formation of the gel within 45 minutes. Primary cardiac cells were diluted in CM at 2 million cells/mL and plated in 2mL of CM for each plate after the gel was fully formed. The cells were cultured in an incubator at 37°C supplied with 5% CO_2 and underwent media changes every other day.

2.8 Contractile Properties Assessment

The cardiac tissues were maintained in culture for 7 to 9 days [Fig. 5(a)] whereupon the constructs were then loaded into the bioreactor to administer mechanical stimulation. Contractile force was measured subsequent to the stimulation protocol being implemented. To measure the contractile force of the bioengineered muscle a highly sensitive TRI202PAD microforce transducer was used (Panlab, Barcelona, Spain) [Fig. 5(b)]. A thin rigid wire was used to attach the tissues to the force transducer. This allows for minimal damage to the construct, while minimizing the amount of force lost due to vibration. The wire is attached at approximately the same point before and after stretching, though some variation may be present. The output signals from the transducer were processed through the PowerLab16/35 data acquisition system (ADInstruments, Colorado Springs, CO), and then transmitted to LabChart for analysis. LabChart's peak analysis feature was used to calculate the maximum twitch force before and after the stretching protocol.

2.9 Attachment of the Cardiac Tissue onto Bioreactor

After the tissues constructs were fully formed, each specimen was loaded onto the bioreactor individually [Fig. 6(a)]. First, the 35mm plate was placed into the bioreactor well. Second, two adjacent minutien pins were removed to allow stretching of the tissue construct. Third, the hooks attached to the bioreactor were placed into the tissue construct on the side where the pins were removed [Fig. 6(b)] to provide unilateral stretching.

The hooks are composed of 20 gauge braided copper wire, soldered to 26 gauge enamel covered solid copper wire, which came into direct contact with the tissue at three equidistant locations. The attachment hooks were sterilized with 80% ethanol before and after each use.

2.10 Mechanical Stimulation Protocol

For the purpose of demonstrating the functionality of the bioreactor, 10 cardiac tissue constructs were loaded onto the bioreactor and stimulated once for a 4 hour period with a pre-established protocol at a frequency of 1Hz with 10% stretch [50] as shown in figure 7(a). The twitch force of each construct was evaluated before and after the stimulation protocol was implemented in order to determine the effect of the mechanical stimulation provided.

2.11 Immunohistochemistry

Samples of the controls and stretched bioengineered tissues were directly fixed in −20°C acetone for 10 minutes. Next, nonspecific epitope antigens were blocked by using 10% goat serum for 1 hour at room temperature. The tissue sections were incubated with mouse anti-α-actinin monoclonal antibody (1:200, Sigma, A7811), rabbit anti-connexin 43 polyclonal antibody (1:100, Abcam, Ab11370), and rabbit anti-collagen type I monoclonal antibody (1:100, EMD Millipore, AB755P) for 2 hours at room temperature. Subsequently, the tissue segments were treated with both goat anti-mouse and goat anti-rabbit secondary antibodies 1:400 (Alexa Fluor 488 and Alexa Fluor 546; Life Technologies, Grand Island, NY) for 1 hour at room temperature. Nuclei were counterstained with 2.5μg/mL 4,6-diamidino-2-phenylindole (DAPI) for 5 minutes at room temperature. The tissue samples were placed on

VWR® Microslides and fluorescent images were produced using a Nikon C2+ confocal laser-scanning microscope (Nikon Instruments Inc., Melville, NY).

3. Results

The bioreactor developed for this study was composed of materials that permitted continuous use of the system inside a cell culture incubator without damaging its components. With this stretch bioreactor we demonstrated the feasibility of providing our muscle constructs with cyclical mechanical stimulation during culture without the need of physically transferring the tissues to the bioreactor. Although only one 35mm culture plate may be loaded into the bioreactor at a time, this design permits the use of different attachment mechanisms to suit a variety of needs. Because the data in this paper was collected using a single bioreactor, the culture time among the tissues varied between 2 to 3 days. This can directly equate to a wider range of twitch force among controls and tissues before stretching. In order to ensure that the tissue constructs suffered little to no damage during testing, slight modifications had to be made to the attachment hooks. Initially, the hooks were made with 22 gauge solid tin wire; nonetheless, this resulted in tearing of the tissues. Once a more suitable attachment method was established, practical data was obtained.

During 3D-AHM fabrication, we observed that the delamination process began 3 days after cell plaiting, once the tissues began to spontaneously contract, and was completed within 2 days. In a previously completed study, we documented the changes in contractile performance of 3D-AHM with a plating density of 2-million cells/construct over the span of two weeks [Fig. 7(b)]. We noted that the constructs were able to maintain contractile performance for a period of 8 days, after which, a significant decrease in performance was observed. These results allowed us to determine at which point in culture the tissue constructs would most likely exhibit a decrease in the contractile properties, in order to provide stimulation at this point. During this study the contractile performance was measured following the implementation of the mechanical stimulation protocol to determine the system's effectiveness. Our study was designed primarily to test our system and obtain preliminary results as to its effect on engineered tissue constructs once they reach a phase where contractile performance begins to decrease. We engineered a total of 10 3D-AHM constructs for mechanical stimulation. However, 3 tissue constructs had to be discarded due to failure before or during the mechanical stimulation. The contractile force recorded for both the controls and tissues before stretching was found to be in the range of 140–2400μN. Due to the wide range of force values obtained, we based our calculations in the overall change seen before and after the 4-hour testing. The overall change in force recorded for stretched tissues was 217.5 ± 150μN and that for non-stretched was −11.5 ± 26.5μN ($p<0.01$). Therefore, the tissues showed an increase in mechanical performance despite the short stimulation period, contrary to the non-stretched constructs [Fig. 7(c)–(e)]. Moreover, we calculated the average force per cross-sectional area for tissues before and after stretching. The average force for tissues before stimulation was found to be 0.0012mN/mm^2, while that after stretching was 0.00160012mN/mm^2. No significant change in construct size after the stretching period was noted (data not shown). In addition, we noted slight tearing of

the cardiac constructs at the point of contact with the stretch attachments. This issue will be addressed in subsequent studies.

Histological data from the bioengineered 3D-AHM was acquired after approximately 2–3 days after mechanical stimulation. The control group and stretched tissues were stained to evaluate the presence of α-actinin, connexin 43, and collagen type I, as shown in figure 8. Positive staining for α-actinin shows the presence of the z-lines of cardiac myofibrils. Stretched tissues [Fig. 8(f)] showed enhanced alignment and longitudinal orientation as a result of the mechanical stimulation. However, the non-stretched tissues [Fig. 8(b)] showed poor alignment. Positive staining for connexin 43 confirms the presence of gap junctions in the fabricated tissue. The presence of gap junctions appears to be higher in stretched tissues [Fig. 8(g)] than in the controls [Fig. 8(c)]. Lastly, positive staining for collagen type I indirectly shows the inhabitance of cardiac fibroblasts within the bioengineered tissue. The results obtained show a slightly better distribution of collagen in stretch construct [Fig. 8(h)] compared to non-stretched [Fig. 8(d)].

4. Discussion

The heart is an intricate system that is incapable of self-repair following lost functionality due to myocardial infarction. Heart muscle tissue engineering focuses on alleviating such issues by providing the latest methodology for fabricating native tissue equivalents. The ultimate goal of which is to produce constructs that resemble native mammalian tissue in function and structure to repair, replace or even augment infarcted tissues. Developing phenotypically and physiologically relevant tissues requires us to mimic conditions found in-vivo using different types of bioreactors. The research described in this manuscript was designed to evaluate the compatibility of a completely novel cyclic strain bioreactor with 3D-AHM developed in our laboratory, as well as to evaluate the initial effect of short-term mechanical stimulation administered to our tissues during the culture and maturation process.

Our system stands out from previously developed bioreactors due to the use of a voice coil actuator. For our application, voice actuators have several advantages over typical linear motors. There are several types of common linear motors used in industry, but most often in tissue engineering these take the form of stepper-motor driven power screws. Linear motors of this type generate vibration during stepping, even when micro-step drivers are used. We have built and used many of this type of linear stepper motors, and have extensive experience with them. To begin with, stepper motor driven actuators have bandwidth limits that would prevent experiments with higher cyclic rates that we are planning for future experiments. The general design approach to overcome the bandwidth limit is to increase the displacement-per-step, which reduces the mechanical displacement resolution as well as increasing the problems associated with using discrete rather than smooth (analog) displacement mechanisms, and because in any design, stepper motors are inherently discrete displacement (step) devices. They often cause vibration in the culture system that is visible as ripples on the culture medium surface and sometimes can be seen with the naked eye as violent shaking of the tissue specimen itself. Moreover, these actuators are prone to resonant vibrations in certain frequencies in the ranges commonly used, so velocity ramps can have

one or more resonance points where the shaking is particularly violent. We have run pilot experiments (not published) to determine whether vibration of this type has an effect on engineered tissues, and in our experience it always has some amount of negative effect on the survivability and development of the engineered tissues. We therefore believe the mechanical behavior inherent in stepper-motor-driven actuators causes damage to engineered tissue specimens, so our new VCA motor design was developed specifically to overcome these limitations. The use of a VCA motor in any case is a much simpler, compact, and efficient solution than resorting to the many questionably effective methods that have been tried over the years to smooth out the discrete steps in stepper-motor-driven actuators. By developing our own system we sought to construct a bioreactor that could easily provide mechanical stimulation to our bioengineered heart muscle as well as measure their contractile force. The structure of our bioreactor allows us to use various types of attachments to suit different types of myocardial constructs. The custom nature of this bioreactor also supports a variety of stretching protocols. For our purposes and the scope of this manuscript, only the cyclical mechanical 10% stretch at 1Hz was used. Other capabilities of the system will be evaluated in future studies.

The initial development of the 3D-AHM starts with the isolation of neonatal rat primary cardiac cells, which are then plated on a fibrin gel. After the delamination process is complete, typically over 4–5 days, the 20x20mm square myocardial patch is fully formed, the shape of which is delineated by the layout of four minutien pins that serve as anchor points for the gel to form around. We chose to provide mechanical stimulation to the constructs once they reached around the 6–8-day mark. It is at this stage when the contractile forces generated by the patches begin to diminish steadily. Testing at this phase of patch development allows us to not only measure the effect of the stretching protocols but also to test if the contractile strength could be maintained over longer periods of time.

We chose to implement a shorter stimulation protocol than previously used to test the compatibility of the system with the tissues, and also to acquire initial data as to the effect of cyclical strain provided with the new system on overall contractile performance. In future studies the long-term effect of stretch on 3D-AHM will be evaluated to establish an ideal protocol for the development and maturation of our cardiac constructs. In addition a more durable and suitable attachment needs to be manufactured to prevent tearing during longer stretching periods.

We have documented that the effect of our 4-hour stretch protocol yielded increases in contractile performance between 1.5–4 fold. More specifically, we observed an overall twitch force increase of 217.5 ± 150μN (~1.5 fold) in stimulated tissues. The discongruity in the change in force after stretching could be attributed not only to the wide initial force range, variations between tissue construct batches, and attachment of the force transducer, but also to the difference in culture time before testing. To alleviate the complications that may arise from the differences in culture time, it is pertinent to manufacture replicates of the bioreactor to be able to test several tissues simultaneously. Furthermore, the unilateral strain provided to the tissues can lead to a less uniform stimulation, accounting for some of the disparity seen in contractile force after strain is applied. In order to mitigate this problem the next attachment mechanism developed must be capable of securing two sides of the tissue,

while maintaining the same distance between connection points to minimize variation between different strain tests. To compare these results with other published works, Akhyari et al. demonstrated that cyclical mechanical stress at 20% stretch and 80 cycles/min resulted in improved tensile strength [45]. Furthermore, a study published by Fink et al. proved improvement of contractile force of engineered heart tissue by 2 to 4 fold with 20% stretch and 1.5Hz [46]. During this study we have proved that the system is capable of improving contractile force, thus validating the system and allowing us to move toward establishing a long-term protocol for future studies.

Immunohistochemical characterization was performed to confirm the presence of cardiac markers in 3D-AHM, as well as to study the effect of cyclic strain on their expression. The results acquired show a well-organized filament network [fig. 8(f)] that provides structural stability to the constructs in response to the cyclic strain. The apparent increase in cardiac gap junction expression in stretched tissues [Fig. 8(g)] may help explain the improved contractile forces seen after mechanical stimulation. With higher presence of gap junctions, electromechanical coupling increases, yielding a more uniform impulse propagation and thus a stronger and more uniform contraction. Additionally, positive staining for collagen type 1 shows the inhabitance of fibroblasts with cardiomyocytes, which can serve as supporting cells. A newly published manuscript on the optimization of 3D-AHM fabricated at our laboratory depicts the effect of these supporting cells in tissue development [54]. Moreover, the more even distribution of collagen seen in the stretched constructs [Fig. 8(h)] may also help explain the increase in force. While fibroblasts contribute to myocardial tissue structure, they are also direct contributors to the tissue's intrinsic electrical properties. Fibroblasts are non-excitable cells that are capable of working as "mechano-electrical transducers" [55], a better distribution can ultimately lead to more synchronous beating, and in return a higher force of contraction. Further testing as to the effect of mechanical stimulation on α-actinin, connexin 43, and collagen type I expression needs to be performed in subsequent longer-term studies to corroborate the results obtained in this study.

We believe that this study has shown the feasibility of using the current bioreactor to sustain the viability of bioengineered heart muscle, as well as improving their overall contractile performance. However, in future studies some of the problems encountered during this study need to be addressed in detail. First, it may be relevant to extend the system to be loaded with several specimens simultaneously to procure more data and to provide consistent mechanical stimulation, as well as mitigate inconsistencies from one test to another. Second, the ability of the bioreactor to directly measure twitch force and tensile strength, as well as generate stress-strain curves needs to be assessed. Third, a more suitable attachment mechanism that provides more uniform stretch is needed. Lastly, we need to perform long-term studies to develop a stretch protocol to be using during cardiac tissue development.

5. Conclusion

A novel programmable bioreactor was manufactured to mechanically stimulate and assess fabricated heart muscle. Compatibility with the tissue samples was experimentally confirmed by assessing damage caused to constructs, the increase in contractile properties, increase in cell alignment, and improved expression of cardiac markers. Preliminary results

obtained in this study suggests that 10% cyclic mechanical stretch at 1Hz can increase the twitch force of the tissues, and maintain their viability for longer periods of time.

References

1. Roger VL, Go AS, Lloyd-Jones DM, Benjamin EJ, Berry JD, Borden WB, et al. Heart Disease and Stroke Statistics-2012 Update: A Report From the American Heart Association. Circulation. 2012; 125(1):e2–e220.10.1161/Cir.0b013e3182456d46 [PubMed: 22179539]
2. Guyton, AC.; Hall, JE. Textbook of medical physiology. 11. Philadelphia: Elsevier Saunders; 2006. p. 27-42.
3. Radisic, M.; Christman, KL., editors. Mayo Clin Proc. 2013 Aug. Materials science and tissue engineering: repairing the heart; p. 3786696
4. Segers VF, Lee RT. Stem-cell therapy for cardiac disease. Nature. 2008; 451(7181):937–42.10.1038/nature06800 [PubMed: 18288183]
5. Beltrami AP, Barlucchi L, Torella D, Baker M, Limana F, Chimenti S, et al. Adult cardiac stem cells are multipotent and support myocardial regeneration. Cell. 2003; 114(6):763–76. [PubMed: 14505575]
6. Laugwitz KL, Moretti A, Lam J, Gruber P, Chen Y, Woodard S, et al. Postnatal isl1+ cardioblasts enter fully differentiated cardiomyocyte lineages. Nature. 2005; 433(7026):647–53.10.1038/nature03215 [PubMed: 15703750]
7. Messina E, De Angelis L, Frati G, Morrone S, Chimenti S, Fiordaliso F, et al. Isolation and expansion of adult cardiac stem cells from human and murine heart. Circulation research. 2004; 95(9):911–21.10.1161/01.RES.0000147315.71699.51 [PubMed: 15472116]
8. Oh, H.; Bradfute, SB.; Gallardo, TD.; Nakamura, T.; Gaussin, V.; Mishina, Y., et al., editors. Proc Natl Acad Sci U S A. 2003 Oct. Cardiac progenitor cells from adult myocardium: homing, differentiation, and fusion after infarction; p. 218755
9. Bergmann O, Bhardwaj RD, Bernard S, Zdunek S, Barnabe-Heider F, Walsh S, et al. Evidence for cardiomyocyte renewal in humans. Science. 2009; 324(5923):98–102.10.1126/science.1164680 [PubMed: 19342590]
10. Bowen FW, Jones SC, Narula N, St John Sutton MG, Plappert T, Edmunds LH Jr, et al. Restraining acute infarct expansion decreases collagenase activity in borderzone myocardium. The Annals of thoracic surgery. 2001; 72(6):1950–6. [PubMed: 11791588]
11. Enomoto Y, Gorman JH 3rd, Moainie SL, Jackson BM, Parish LM, Plappert T, et al. Early ventricular restraint after myocardial infarction: extent of the wrap determines the outcome of remodeling. The Annals of thoracic surgery. 2005; 79(3):881–7. discussion -7. 10.1016/j.athoracsur.2004.05.072 [PubMed: 15734399]
12. Kelley ST, Malekan R, Gorman JH 3rd, Jackson BM, Gorman RC, Suzuki Y, et al. Restraining infarct expansion preserves left ventricular geometry and function after acute anteroapical infarction. Circulation. 1999; 99(1):135–42. [PubMed: 9884390]
13. Moainie SL, Guy TS, Gorman JH 3rd, Plappert T, Jackson BM, St John-Sutton MG, et al. Infarct restraint attenuates remodeling and reduces chronic ischemic mitral regurgitation after postero-lateral infarction. The Annals of thoracic surgery. 2002; 74(2):444–9. discussion 9. [PubMed: 12173827]
14. Pilla JJ, Blom AS, Brockman DJ, Ferrari VA, Yuan Q, Acker MA. Passive ventricular constraint to improve left ventricular function and mechanics in an ovine model of heart failure secondary to acute myocardial infarction. J Thorac Cardiovasc Surg. 2003; 126(5):1467–75. [PubMed: 14666021]
15. Christman KL, Fok HH, Sievers RE, Fang QH, Lee RJ. Fibrin glue alone and skeletal myoblasts in a fibrin scaffold preserve cardiac function after myocardial infarction. Tissue engineering. 2004; 10(3–4):403–9.10.1089/107632704323061762 [PubMed: 15165457]
16. Christman KL, Vardanian AJ, Fang Q, Sievers RE, Fok HH, Lee RJ. Injectable fibrin scaffold improves cell transplant survival, reduces infarct expansion, and induces neovasculature formation in ischemic myocardium. Journal of the American College of Cardiology. 2004; 44(3):654–60.10.1016/j.jacc.2004.04.040 [PubMed: 15358036]

17. Huang NF, Yu J, Sievers R, Li S, Lee RJ. Injectable biopolymers enhance angiogenesis after myocardial infarction. Tissue engineering. 2005; 11(11–12):1860–6.10.1089/ten.2005.11.1860 [PubMed: 16411832]
18. Kofidis T, Lebl DR, Martinez EC, Hoyt G, Tanaka M, Robbins RC. Novel injectable bioartificial tissue facilitates targeted, less invasive, large-scale tissue restoration on the beating heart after myocardial injury. Circulation. 2005; 112(9 Suppl):I173–7.10.1161/CIRCULATIONAHA.104.526178 [PubMed: 16159811]
19. Ryu JH, Kim IK, Cho SW, Cho MC, Hwang KK, Piao H, et al. Implantation of bone marrow mononuclear cells using injectable fibrin matrix enhances neovascularization in infarcted myocardium. Biomaterials. 2005; 26(3):319–26.10.1016/j.biomaterials.2004.02.058 [PubMed: 15262474]
20. Christman KL, Lee RJ. Biomaterials for the treatment of myocardial infarction. Journal of the American College of Cardiology. 2006; 48(5):907–13.10.1016/j.jacc.2006.06.005 [PubMed: 16949479]
21. Leor J, Aboulafia-Etzion S, Dar A, Shapiro L, Barbash IM, Battler A, et al. Bioengineered cardiac grafts: A new approach to repair the infarcted myocardium? Circulation. 2000; 102(19 Suppl 3):III56–61. [PubMed: 11082363]
22. Miyahara Y, Nagaya N, Kataoka M, Yanagawa B, Tanaka K, Hao H, et al. Monolayered mesenchymal stem cells repair scarred myocardium after myocardial infarction. Nature medicine. 2006; 12(4):459–65.10.1038/nm1391
23. Shimizu T, Yamato M, Isoi Y, Akutsu T, Setomaru T, Abe K, et al. Fabrication of pulsatile cardiac tissue grafts using a novel 3-dimensional cell sheet manipulation technique and temperature-responsive cell culture surfaces. Circulation research. 2002; 90(3):e40. [PubMed: 11861428]
24. Zimmermann WH, Didie M, Wasmeier GH, Nixdorff U, Hess A, Melnychenko I, et al. Cardiac grafting of engineered heart tissue in syngenic rats. Circulation. 2002; 106(12 Suppl 1):I151–7. [PubMed: 12354725]
25. Zimmermann WH, Eschenhagen T. Cardiac tissue engineering for replacement therapy. Heart failure reviews. 2003; 8(3):259–69. [PubMed: 12878835]
26. Zimmermann WH, Melnychenko I, Wasmeier G, Didie M, Naito H, Nixdorff U, et al. Engineered heart tissue grafts improve systolic and diastolic function in infarcted rat hearts. Nature medicine. 2006; 12(4):452–8.10.1038/nm1394
27. Birla, R. The IEEE Press Series on Biomedical Engineering. Wiley; 2014. Introduction to tissue engineering: applications and challenges.
28. Birla RK, Borschel GH, Dennis RG, Brown DL. Myocardial engineering in vivo: formation and characterization of contractile, vascularized three-dimensional cardiac tissue. Tissue engineering. 2005; 11(5–6):803–13.10.1089/ten.2005.11.803 [PubMed: 15998220]
29. Hecker L, Birla RK. Engineering the heart piece by piece: state of the art in cardiac tissue engineering. Regenerative medicine. 2007; 2(2):125–44.10.2217/17460751.2.2.125 [PubMed: 17465746]
30. Vunjak-Novakovic G, Tandon N, Godier A, Maidhof R, Marsano A, Martens TP, et al. Challenges in cardiac tissue engineering. Tissue engineering Part B, Reviews. 2010; 16(2):169–87.10.1089/ten.TEB.2009.0352 [PubMed: 19698068]
31. Baar K, Birla R, Boluyt MO, Borschel GH, Arruda EM, Dennis RG. Self-organization of rat cardiac cells into contractile 3-D cardiac tissue. The FASEB Journal. 2004
32. Blan NR, Birla RK. Design and fabrication of heart muscle using scaffold-based tissue engineering. J Biomed Mater Res A. 2008; 86A(1):195–208.10.1002/Jbm.A.31642 [PubMed: 17972281]
33. Evers R, Khait L, Birla RK. Fabrication of functional cardiac, skeletal, and smooth muscle pumps in vitro. Artificial organs. 2011; 35(1):69–74.10.1111/j.1525-1594.2010.01007.x [PubMed: 20618224]
34. Huang YC, Khait L, Birla RK. Contractile three-dimensional bioengineered heart muscle for myocardial regeneration. J Biomed Mater Res A. 2007; 80(3):719–31.10.1002/jbm.a.31090 [PubMed: 17154158]

35. Khait L, Hodonsky CJ, Birla RK. Variable optimization for the formation of three-dimensional self-organized heart muscle. In vitro cellular & developmental biology. Animal. 2009; 45(10): 592–601.10.1007/s11626-009-9234-1
36. Migneco F, Hollister SJ, Birla RK. Tissue-engineered heart valve prostheses: 'state of the heart'. Regenerative medicine. 2008; 3(3):399–419.10.2217/17460751.3.3.399 [PubMed: 18462061]
37. Akins RE, Boyce RA, Madonna ML, Schroedl NA, Gonda SR, McLaughlin TA, et al. Cardiac organogenesis in vitro: reestablishment of three-dimensional tissue architecture by dissociated neonatal rat ventricular cells. Tissue engineering. 1999; 5(2):103–18. [PubMed: 10358218]
38. Carrier RL, Papadaki M, Rupnick M, Schoen FJ, Bursac N, Langer R, et al. Cardiac tissue engineering: cell seeding, cultivation parameters, and tissue construct characterization. Biotechnol Bioeng. 1999; 64(5):580–9. [PubMed: 10404238]
39. Sachs HG, DeHaan RL. Embryonic myocardial cell aggregates: volume and pulsation rate. Developmental biology. 1973; 30(1):233–40. [PubMed: 4697746]
40. Shimizu T, Sekine H, Yamato M, Okano T. Cell sheet-based myocardial tissue engineering: new hope for damaged heart rescue. Current pharmaceutical design. 2009; 15(24):2807–14. [PubMed: 19689351]
41. Shimizu T, Yamato M, Akutsu T, Shibata T, Isoi Y, Kikuchi A, et al. Electrically communicating three-dimensional cardiac tissue mimic fabricated by layered cultured cardiomyocyte sheets. Journal of biomedical materials research. 2002; 60(1):110–7. [PubMed: 11835166]
42. Shimizu T, Yamato M, Kikuchi A, Okano T. Two-dimensional manipulation of cardiac myocyte sheets utilizing temperature-responsive culture dishes augments the pulsatile amplitude. Tissue engineering. 2001; 7(2):141–51.10.1089/107632701300062732 [PubMed: 11304450]
43. Shimizu T, Yamato M, Kikuchi A, Okano T. Cell sheet engineering for myocardial tissue reconstruction. Biomaterials. 2003; 24(13):2309–16. [PubMed: 12699668]
44. Zimmermann WH, Schneiderbanger K, Schubert P, Didie M, Munzel F, Heubach JF, et al. Tissue engineering of a differentiated cardiac muscle construct. Circulation research. 2002; 90(2):223–30. [PubMed: 11834716]
45. Akhyari P, Fedak PWM, Weisel RD, Lee TYJ, Verma S, Mickle DAG, et al. Mechanical stretch regimen enhances the formation of bioengineered autologous cardiac muscle grafts. Circulation. 2002; 106(13):I137–I42.10.1161/01.Cir.0000032893.55215.Fc [PubMed: 12354723]
46. Fink C, Ergun S, Kralisch D, Remmers U, Weil J, Eschenhagen T. Chronic stretch of engineered heart tissue induces hypertrophy and functional improvement. Faseb J. 2000; 14(5):669–79. [PubMed: 10744624]
47. Schaaf S, Shibamiya A, Mewe M, Eder A, Stohr A, Hirt MN, et al. Human Engineered Heart Tissue as a Versatile Tool in Basic Research and Preclinical Toxicology. Plos One. 2011; 6(10):ARTN e26397.10.1371/journal.pone.0026397
48. Tulloch NL, Muskheli V, Razumova MV, Korte FS, Regnier M, Hauch KD, et al. Growth of Engineered Human Myocardium With Mechanical Loading and Vascular Coculture. Circulation research. 2011; 109(1):47–U195.10.1161/Circresaha.110.237206 [PubMed: 21597009]
49. Zimmermann WH, Schneiderbanger K, Schubert P, Didie M, Munzel F, Heubach JF, et al. Tissue engineering of a differentiated cardiac muscle construct. Circulation research. 2002; 90(2):223–30.10.1161/Hh0202.103644 [PubMed: 11834716]
50. Birla RK, Huang YC, Dennis RG. Development of a novel bioreactor for the mechanical loading of tissue-engineered heart muscle. Tissue engineering. 2007; 13(9):2239–48.10.1089/Ten.2006.0359 [PubMed: 17590151]
51. Holden JK, Nguyen RH, Francisco EM, Zhang Z, Dennis RG, Tommerdahl M. A novel device for the study of somatosensory information processing. J Neurosci Meth. 2012; 204(2):215–20.10.1016/J.Jneumeth.2011.11.007
52. Halliday, D.; Robert, R.; Walker, J. Electromagnetism and Optics. 7. John Wiley & Sons Inc; 2006. p. 764-816.
53. Dennis, RG. Measurement of pulse propagation in single permeabilized muscle fibers by optical diffraction. Ann Arbor, MI: University of Michigan; 1996.

54. Tao ZW, Mohamed M, Hogan M, Gutierrez L, Birla RK. Optimizing a spontaneously contracting heart tissue patch with rat neonatal cardiac cells on fibrin gel. Journal of tissue engineering and regenerative medicine. 201410.1002/term.1895

55. Camelliti P, Borg TK, Kohl P. Structural and functional characterisation of cardiac fibroblasts. Cardiovasc Res. 2005; 65(1):40–51.10.1016/j.cardiores.2004.08.020 [PubMed: 15621032]

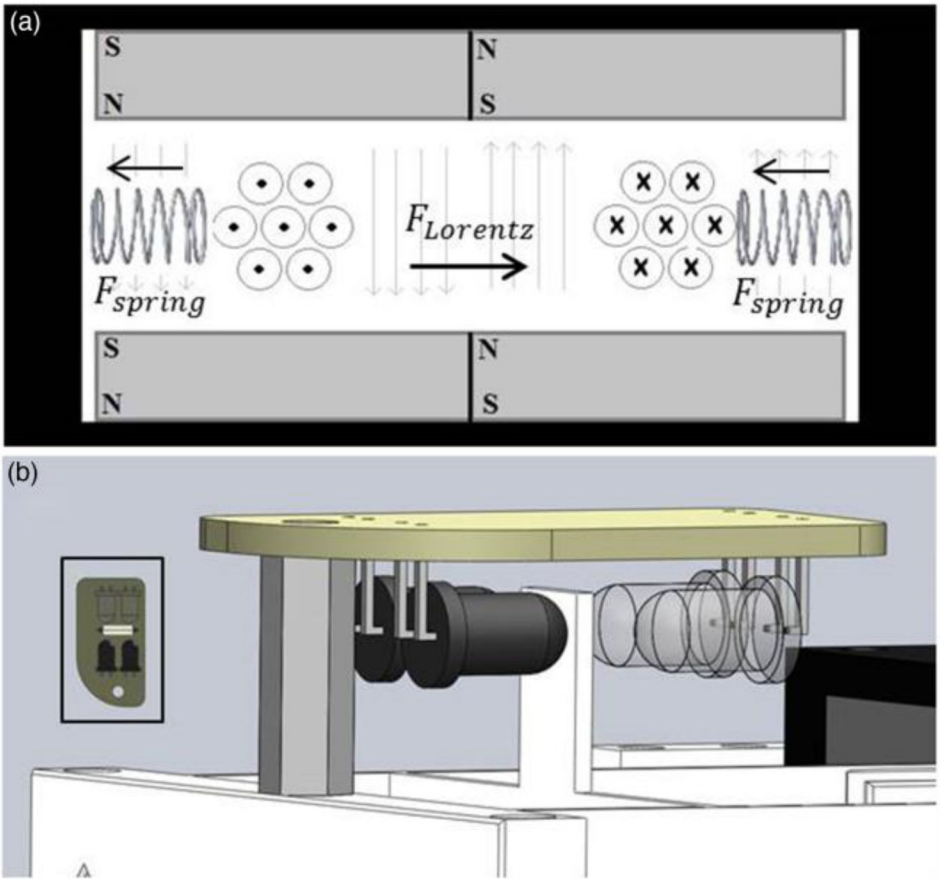

Fig. 1. Design of Bioreactor Operation

(a) Cross-sectional conceptual drawing of the voice coil actuator theory. The direction of current in the coil is depicted conventionally. The springs in this figure represent the effect of the flexible ABS frame. **(b)** Optoelectronic differential position sensor

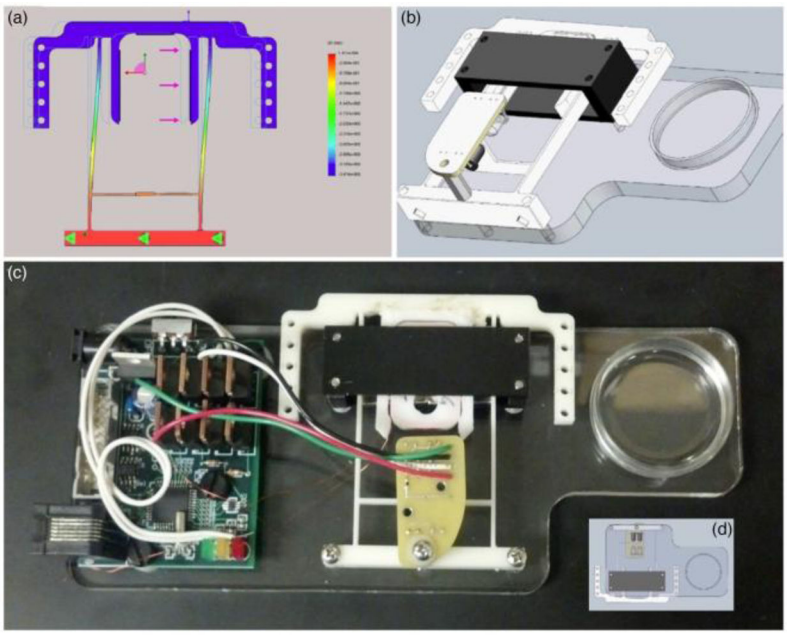

Fig. 2. Design and Structure of Bioreactor

(a) SolidWorks motion study for the design of the flexible frame **(b)** Assembly of the VCA mechanical design **(c)** Image of complete bioreactor hardware **(d)** Inverted view of the SolidWorks Assembly

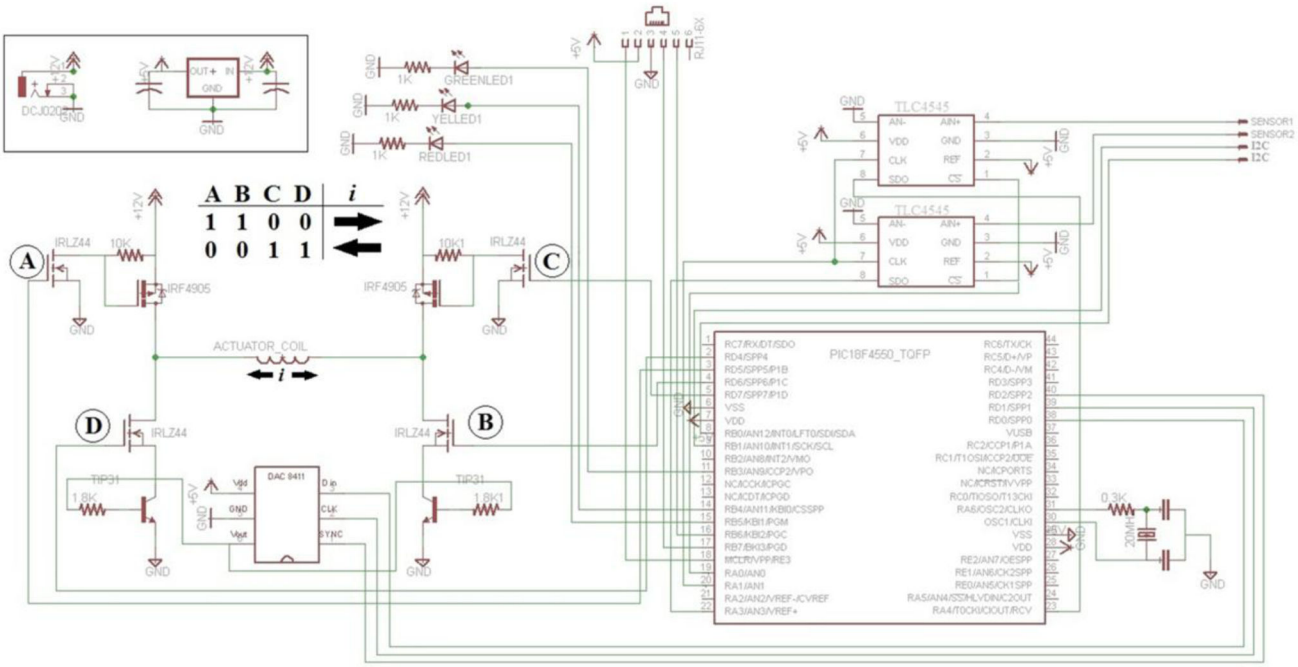

Fig. 3. Printed Circuit Board Design

Circuit schematic for the voice coil actuator driver and control circuitry. The voice coil actuator is driven by a digital H-bridge circuit that consists of N-Ch (IRLZ44) and P-Ch (IRF4905) MOSFETS. The magnitude of the current through the coil to drive the movement of the armature was controlled by a 16-bit analog to digital converter (DAC8411) that was attached to the base of a NPN power transistor (TIP 3055)

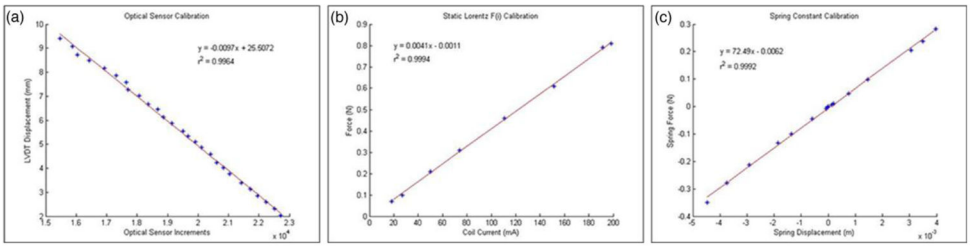

Fig. 4. Bioreactor Calibrations

(a) Calibration of the position sensor against the linearly variable differential transformer (LVDT) **(b)** Calibration of the Lorentz force generated as coil current is varied. **(c)** Armature spring constant calculation using the calibrations of A and B

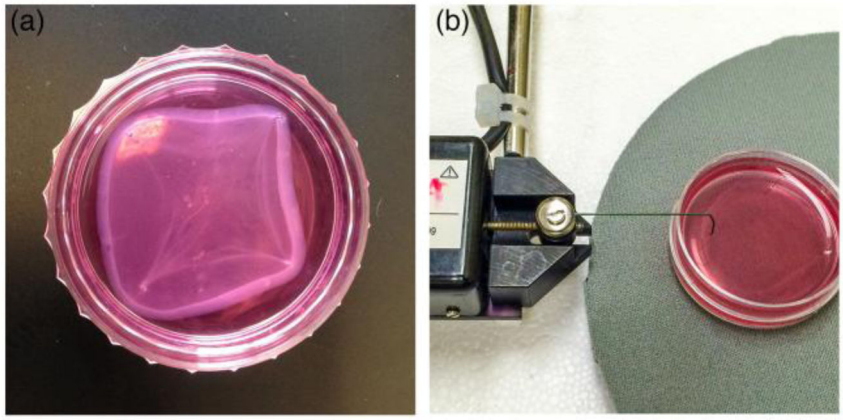

Fig. 5. 3D-AHM and contractile properties assessment

(a) Image showing the fully formed bioengineered muscle. **(b)** Image showing the set up used to determine the contractility of the tissues

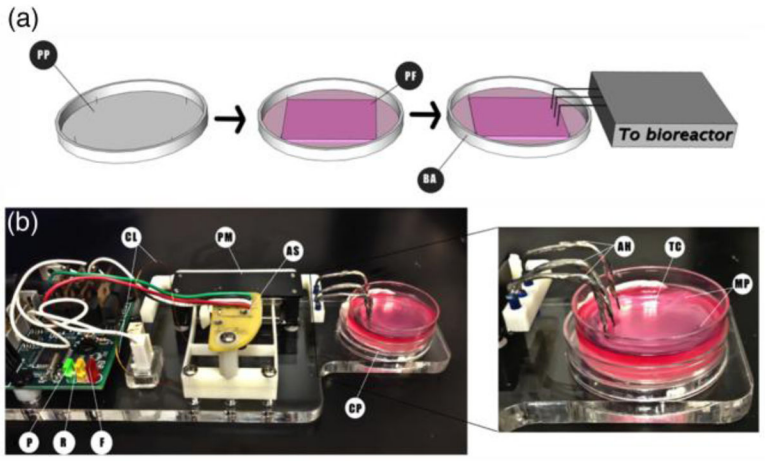

Fig. 6. Patch formation process and setup of the bioreactor for the engineered tissues

(a) Schematic showing the overview of the method used to construct the cardiac tissues. PP: plate preparation, PF: patch formation, BA: bioreactor attachment to tissue construct. **(b)** Setup of the culture plate in the bioreactor and close picture showing the attachment between the device and the tissue construct. CL: coil leads, PM: permanent magnet, AS: armature sensor, P: power LED, F: forward movement LED, R: reverse movement LED, CP: culture plate, AH: attachment Hooks, TC: tissue construct, MP: minutien pins

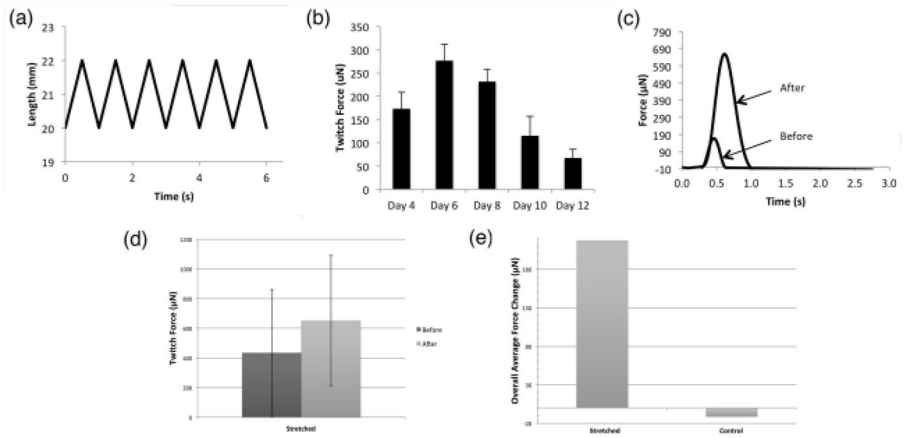

Fig. 7. Mechanical Stimulation and Contractile Performance

(a) Stimulation protocol applied to the constructs for 10% stretch and 1 Hz frequency. **(b)** Changes in the contractile properties over time of cultured tissues, with a plating density of 2 million cells/construct. **(c)** Force tracing of a tissue construct in response to loading when stretched for 4 hours. **(d)** Active force of tissue constructs before and after mechanical stimulation. **(e)** Overall changes in the active force of controls and stretched tissue constructs

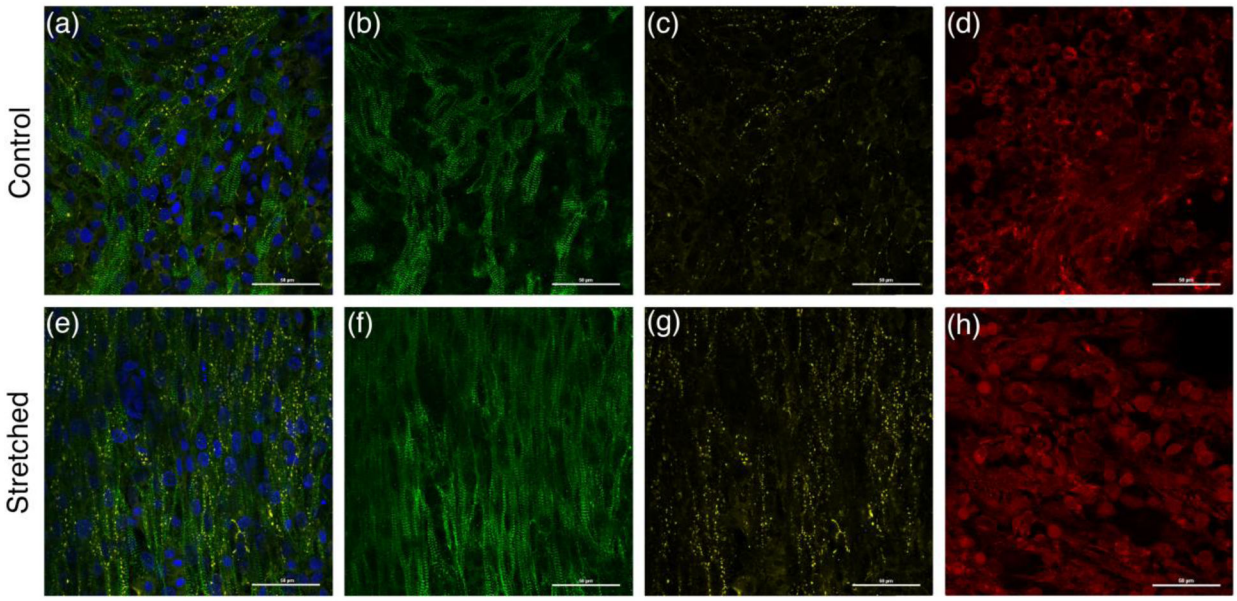

Fig. 8. Immunohistological assessment of fabricated cardiac muscle

(a) Immunofluorescent image showing positive staining for α-actinin (green), connexin 43 (yellow), and collagen type I (red) in non-stretched tissue. **(b)** Immunofluorescent image showing α-actinin expression of control tissues. **(c)** Immunofluorescent image showing connexin 43 expression of stretched tissues. **(d)** Immunofluorescent image showing collagen type I expression of control tissues. **(e)** Immunofluorescent image showing positive staining for α-actinin (green), connexin 43 (yellow), and collagen type I (red) in stretched tissue. **(f)** Immunofluorescent image showing α-actinin expression of stretched tissues. **(g)** Immunofluorescent image showing connexin 43 expression of stretched tissues. **(h)** Immunofluorescent image showing collagen type I expression of stretched tissues